CoAl2O4–Fe2O3 p-n nanocomposite electrodes for photoelectrochemical cells

Kwang-Soon Ahn, Yanfa Yan, Moon-Sung Kang, Jin-Young Kim, Sudhakar Shet et al.

Citation: Appl. Phys. Lett. **95**, 022116 (2009); doi: 10.1063/1.3183585
View online: http://dx.doi.org/10.1063/1.3183585
View Table of Contents: http://apl.aip.org/resource/1/APPLAB/v95/i2
Published by the American Institute of Physics.

$CoAl_2O_4$–Fe_2O_3 *p-n* nanocomposite electrodes for photoelectrochemical cells

Kwang-Soon Ahn,[1,a)] Yanfa Yan,[1,b)] Moon-Sung Kang,[2] Jin-Young Kim,[1] Sudhakar Shet,[1] Heli Wang,[1] John Turner,[1] and Mowafak Al-Jassim[1]
[1]*National Renewable Energy Laboratory, Golden, Colorado 80401, USA*
[2]*Energy and Environment Laboratory, Samsung Advanced Institute of Technology, Yongin-si, Gyeonggi-do 446-712, Republic of Korea*

(Received 26 May 2009; accepted 30 June 2009; published online 17 July 2009)

$CoAl_2O_4$–Fe_2O_3 *p-n* nanocomposite electrodes were deposited on Ag-coated stainless-steel substrates and annealed at 800 °C. Their photoelectrochemical (PEC) properties were investigated and compared with that of *p*-type $CoAl_2O_4$ films. We found that the nanocomposite electrodes exhibit much improved PEC photoresponse as compared to the reference *p*-type $CoAl_2O_4$ electrodes. We speculate that the enhancement is due to the formation of a three-dimensional junction between *p*-type $CoAl_2O_4$ and *n*-type Fe_2O_3 nanoparticles, which improves electron-hole separation, thus reducing charge recombination upon light illumination. © *2009 American Institute of Physics*. [DOI: 10.1063/1.3183585]

Transition-metal-oxide-based photoelectrochemical (PEC) materials for the splitting of water under visible-light illumination has attracted wide interest since the discovery of photoinduced decomposition of water on TiO_2 electrodes.[1–5] To date, most investigations have focused on *n*-type materials such as TiO_2, ZnO, WO_3, and Fe_2O_3 due to their ease of synthesis and their potential stability in aqueous solutions.[1–5] For water splitting, the use of both *n*-type and *p*-type semiconductors is often necessary.[6] Unfortunately, most *p*-type materials that have been identified are susceptible to photocorrosion.[7]

Recently, Woodhouse *et al.*[8,9] and our group[10] reported that the Co-based spinel oxides such as $CoAl_2O_4$ are possible candidates as *p*-type oxide electrodes for PEC water splitting. These *p*-type oxides are found to be very stable in aqueous solution; however, the photoresponses of these oxides was found to be weak.[8,9] It is therefore necessary to develop approaches to enhance their photoresponse.

Like other nanostructures, nanoparticles are often used as an approach to enhance PEC response due to the greatly increased surface areas. The electric field generated in the depletion layer is generally necessary for photovoltaic devices because it helps to separate the photogenerated electron-hole pairs, reducing carrier recombination.[11,12] Thus, attempts to suppress the recombination rate in the nanostructures have been performed by energy-band engineering or developing a *p-n* nanojunction.[13]

In this letter, we discuss our results with *p-n* nanocomposite electrodes consisting of *p*-$CoAl_2O_4$ and *n*-Fe_2O_3 nanoparticles for enhancing the PEC photoresponse. The performance of these *p-n* nanocomposite electrodes is compared with that of *p*-$CoAl_2O_4$ nanoparticles electrodes. All synthesized electrodes exhibited *p*-type behavior and were very resistant to photocorrosion. However, the nanocomposite electrodes exhibited a much improved PEC photoresponse as compared to the reference *p*-type $CoAl_2O_4$ electrodes.

The preparation of $CoAl_2O_4$–Fe_2O_3 *p-n* nanocomposite film electrodes starts from dispersing $CoAl_2O_4$ and Fe_2O_3 nanoparticles (size <50 nm, Sigma-Aldrich Co.) in ethanol by paint shaking for 2 h. Mixed nanoparticles with Fe_2O_3 concentrations from 5 to 20 wt % were prepared. These colloids were thoroughly dispersed using a conditioning mixer by adding ethyl cellulose as the binder and α-terpineol as a solvent for the pastes, followed by concentration using an evaporator. The pastes were doctor-bladed on Ag-coated stainless-steel substrates (Ag/SS), followed by calcination at 800 °C for 4 h in air to remove the binder. All samples have a similar film thickness of about 6 μm as measured by stylus profilometry.

The structural and crystallinity characterizations were performed by x-ray diffraction (XRD). The surface morphology was examined by field-emission scanning electron microscopy (FE-SEM). PEC measurements were performed in a three-electrode cell with a flat quartz window to facilitate illumination of the photoelectrode surface.[14,15] The nanocomposite films and the $CoAl_2O_4$ nanoparticle films (active area: 0.25 cm^2) were used as working electrodes. A Pt sheet (area: 10 cm^2) and an Ag/AgCl electrode (with saturated KCl) were used as counter and reference electrodes, respectively. A 0.5 M NaOH aqueous solution (pH ~ 13) was used as the electrolyte. The light source was a fiber-optic illuminator (150 W tungsten-halogen lamp) with an ultraviolet (UV)/infrared (IR) cutoff filter (350 nm $\geq \lambda \leq$ 750 nm) to highlight the interest in the visible spectrum. The applied light intensity after the UV/IR filter was 75 mW/cm^2, measured with a photodiode power meter.

When *p*-type and *n*-type nanoparticles are well mixed together with good nanoparticle interconnection, a three-dimensional *p-n* junction can be formed. To ensure quality nanoparticle interconnection, the mixed nanoparticle films need to be annealed at high temperature, here 800 °C (below solid reaction temperature). The widely used fluorine-doped tin oxide-coated glass substrate is not suitable for this application because it is thermally unstable at this annealing temperature. We have therefore used Ag/SS as an alternative

[a)]Current address: School of Display and Chemical Engineering, Yeungnam University, Dae-dong, Kyungsan, South Korea 712-749. Electronic mail: kstheory@ynu.ac.kr.
[b)]Electronic mail: yanfa.yan@nrel.gov.

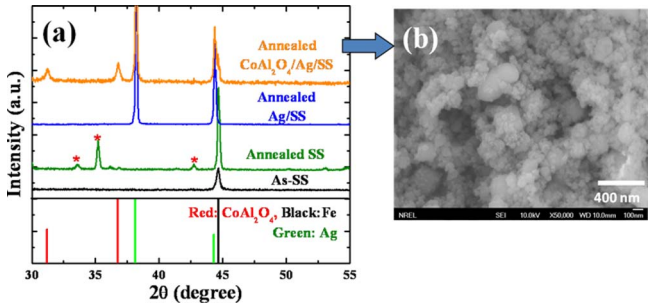

FIG. 1. (Color online) (a) XRD curve of unannealed and annealed SS substrates, annealed Ag/SS substrate, and $CoAl_2O_4$/Ag/SS. (b) SEM image of annealed $CoAl_2O_4$/Ag/SS.

substrate because the solubility of Ag in Fe is extremely small and the melting point of Ag is 960 °C. Figure 1(a) shows XRD patterns for SS and Ag/SS before and after annealing at 800 °C in air. The SS shows the formation of iron oxide (* peaks) on the surface after the annealing, indicating that SS is not appropriate as the substrate for $CoAl_2O_4$ electrodes. This is because iron oxide has very poor electrical conductivity, making it difficult to collect current from the $CoAl_2O_4$ to the SS. On the other hand, Ag/SS exhibited no evidence of formation of oxides after the annealing at 800 °C in air. Therefore, $CoAl_2O_4$–Fe_2O_3 nanocomposite films could be coated on Ag/SS and annealed at 800 °C without substrate deterioration [see the XRD curve of the annealed $CoAl_2O_4$/Ag/SS sample in Fig. 1(a)]. The SEM image shown in Fig. 1(b) indicates that the annealed nanocomposite electrode is nanoporous, and its particle size corresponds well to the crystallite size (33 nm) calculated from the XRD peak around 36.8°. The particle size is also the same as the unannealed particles, indicating that no obvious solid reaction occurred during the annealing.

Figure 2(a) shows the PEC response for a pure $CoAl_2O_4$ nanoparticle electrode under light on/off conditions at −1 V. When the light was on, *cathodic* photocurrents were registered, indicating that $CoAl_2O_4$ is a *p*-type semiconductor. The photocurrent as a function of applied potential (from 0.0 to −1.0 V) is shown in Fig. 2(b). It shows that the onset potential of the photocurrent occurs at −0.2 V and the photocurrent saturates from −0.6 V. The inset in Fig. 2(b) shows the stability of the electrode against photocorrosion when operated at −1 V. It is seen that $CoAl_2O_4$ is very stable in the basic solution, a property not typically seen for *p*-type materials.

Figure 3(a) shows the comparison of PEC responses of a nanocomposite film with 5 wt % Fe_2O_3 and a reference $CoAl_2O_4$ nanoparticle film. Again, the photocurrent is cathodic, meaning that the overall electrode behaves as *p*-type. The saturated photocurrents are lined up for comparison. It shows clearly that the photocurrent with the nanocomposite film is much larger than that with *p*-type $CoAl_2O_4$ nanoparticle film only. Figure 3(b) shows the photocurrents at −1 V for nanocomposite films with different amounts of Fe_2O_3. It is seen that all $CoAl_2O_4$–Fe_2O_3 *p-n* nanocomposite films exhibit much improved PEC responses over the $CoAl_2O_4$ nanoparticle film. However, the enhancement does not increase linearly with the amount of Fe_2O_3 nanoparticles, because too much Fe_2O_3 would lead to a lower amount of *p*-type $CoAl_2O_4$ and less contact area with electrolyte. The highest photocurrent is seen with an Fe_2O_3 content of 5 wt %. Figure 3(c) shows photocurrent measured at −1 V as a function as wavelength for the $CoAl_2O_4$ with 10 wt % Fe_2O_3. It clearly shows that the photoresponse of the nanocomposite film only occurs at the wavelengths less than ~532 nm (2.33 eV), which corresponds to the bandgap of $CoAl_2O_4$, rather than that of Fe_2O_3. This result further indicates that the enhanced photoresponses of nanocomposite films are not due to the contribution from Fe_2O_3, but to the reduced carrier recombination or carrier separation promoted by the three-dimensional *p-n* junction. We also note the very slow response time for these electrodes that is due to the mechanism of charge transport in these materials. Both the pure $CoAl_2O_4$ and the nanocomposite electrodes exhibit slow carrier-transport kinetics due to the large effective masses for both electrons and holes in $CoAl_2O_4$. The *p-n* nanocomposite structure does not address this problem. Suggestions on how to solve this problem will be published elsewhere.[16]

Our hypothesis as to why the $CoAl_2O_4$–Fe_2O_3 *p-n* nanocomposite electrodes exhibit enhanced PEC performance over the $CoAl_2O_4$ nanoparticle films is as follows: when *p*-type $CoAl_2O_4$ and *n*-type Fe_2O_3 nanoparticles are interconnected, a three-dimensional *p-n* junction can form with their valance bands and conduction bands (CBs) offset, as shown in Fig. 3(d). Unlike conventional *p-n* junctions, no

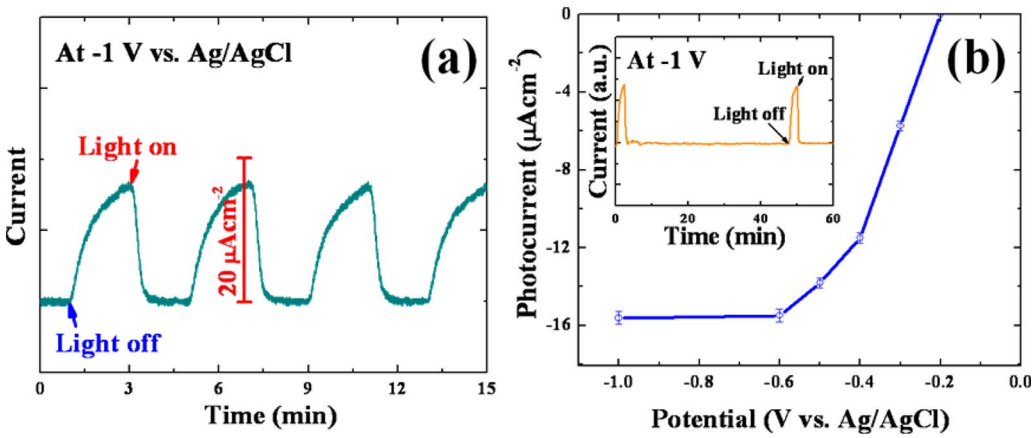

FIG. 2. (Color online) (a) PEC response measured for pure $CoAl_2O_4$ nanoparticle electrode with a time under the light on/off conditions at constant −1 V. (d) Measured *I-V* curve for pure $CoAl_2O_4$ nanoparticle electrode.

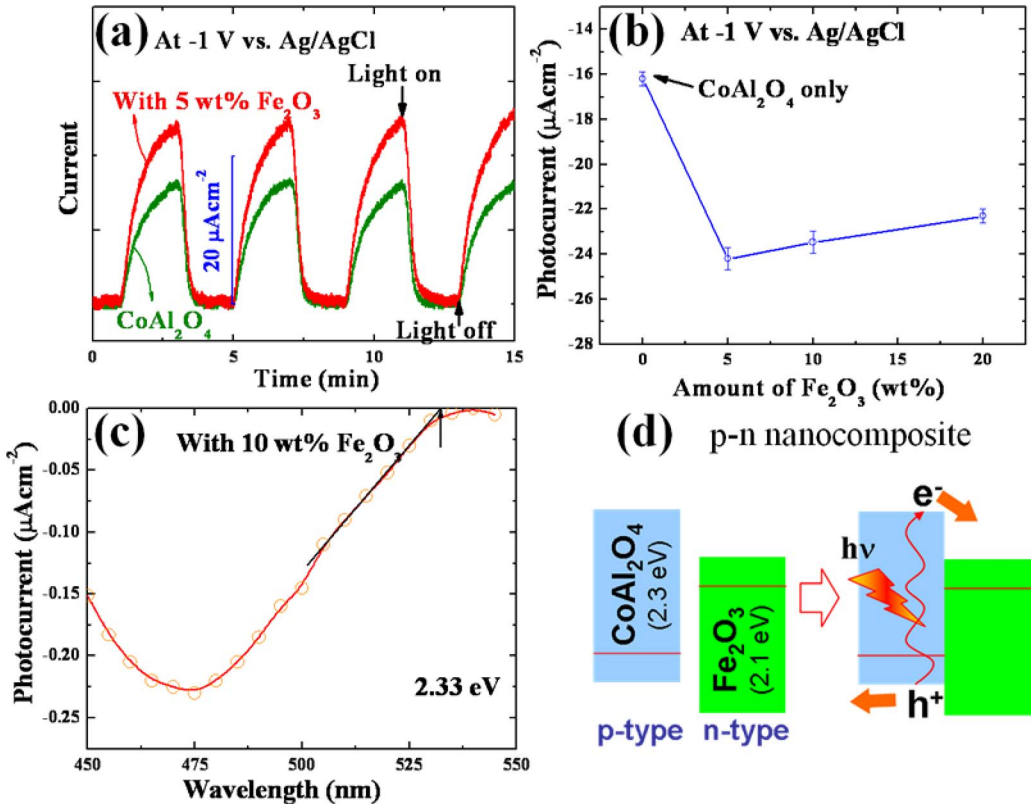

FIG. 3. (Color online) (a) Comparison of PEC responses for pure $CoAl_2O_4$ nanoparticle and *p-n* nanocomposite electrodes under the light on/off conditions at −1 V. (b) Photocurrents at −1 V for nanocomposite films with different amount of Fe_2O_3. (c) Photocurrent at −1 V as a function as incident monochromatic light wavelength for the $CoAl_2O_4$ nanocomposite with 10 wt % Fe_2O_3. (d) Band diagram for *p*-type $CoAl_2O_4$ and *n*-type Fe_2O_3 nanocomposite.

traditional depletion region—and thus, no built-in electrical field—is expected at the $CoAl_2O_4/Fe_2O_3$ and electrode/electrolyte interfaces due to the nanoparticle structure. This built-in electrical field in conventional *p-n* junction usually promotes holes to the *p*-side and electrons to the *n*-side of the junction, which, in this case, is not desirable for water splitting. However, in this case, upon illumination, photogenerated electron-hole pairs will be separated due to the band offset, leading to reduced carrier recombination. Electrons will be injected into Fe_2O_3 and holes will remain in $CoAl_2O_4$. The electron injection will be much faster kinetically than the hydrogen reaction at the $CoAl_2O_4$ surface. Thus, hydrogen will be preferentially evolved at the Fe_2O_3 sites. We speculate that the enhancement on PEC performance is due to the formation of a three-dimensional *p-n* junction, which promotes photogenerated carrier separation and reduces their recombination. However, when an excessively large amount of Fe_2O_3 nanoparticles is added in the film, Fe_2O_3 nanoparticles could shadow the $CoAl_2O_4$ and/or block interparticle hole-transport through nanoporous $CoAl_2O_4$ and thus limit the enhancement of photocurrent.

In summary, $CoAl_2O_4$–Fe_2O_3 *p-n* nanocomposite electrodes were deposited on Ag-coated stainless steel and annealed at 800 °C. We found that the nanocomposite electrodes exhibited much improved photoresponses as compared to *p*-type $CoAl_2O_4$ only. We attribute the improvement to the band offset at the three-dimensional *p-n* junction interface, which promotes photogenerated carrier separation and reduces carrier recombination.

This work is supported by the U.S. Department of Energy (DOE) under Grant No. DE-AC36-08GO28308.

[1] A. Fujishima and K. Honda, Nature (London) **238**, 37 (1972).
[2] O. Khaselev and J. A. Turner, Science **280**, 425 (1998).
[3] J. Yuan, M. Chen, J. Shi, and W. Shangguan, Int. J. Hydrogen Energy **31**, 1326 (2006).
[4] B. O'Regan and M. Grätzel, Nature (London) **353**, 737 (1991).
[5] T. F. Jaramillo, S. H. Baeck, A. Kleiman-Shwarsctein, and E. W. McFarland, Macromol. Rapid Commun. **25**, 297 (2004).
[6] A. J. Nozik, Appl. Phys. Lett. **29**, 150 (1976).
[7] G. K. Mor, O. K. Varghese, R. H. T. Wilke, S. Sharma, K. Shankar, T. J. Latempa, K.-S. Choi, and C. A. Grimes, Nano Lett. **8**, 1906 (2008).
[8] M. Woodhouse, G. S. Herman, and B. A. Parkinson, Chem. Mater. **17**, 4318 (2005).
[9] M. Woodhouse and B. A. Parkinson, Chem. Mater. **20**, 2495 (2008).
[10] A. Walsh, S.-H. Wei, Y. Yan, M. M. Al-Jassim, and J. A. Turner, Phys. Rev. B **76**, 165119 (2007).
[11] G. Schlichthörl, S. Y. Huang, J. Sprague, and A. J. Frank, J. Phys. Chem. B **101**, 8141 (1997).
[12] R. Beranek, H. Tsuchiya, T. Sugishima, J. M. Macak, L. Taveira, S. Fujimoto, H. Kisch, and P. Schmuki, Appl. Phys. Lett. **87**, 243114 (2005).
[13] H. G. Kim, P. H. Borse, W. Choi, and J. S. Lee, Angew. Chem., Int. Ed. **44**, 4585 (2005).
[14] K.-S. Ahn, Y. Yan, S.-H. Lee, T. Deutsch, J. Turner, C. E. Tracy, C. Perkins, and M. Al-Jassim, J. Electrochem. Soc. **154**, B956 (2007).
[15] K.-S. Ahn, Y. Yan, S. Shet, T. Deutsch, K. Jones, J. Turner, and M. Al-Jassim, Appl. Phys. Lett. **93**, 163117 (2008).
[16] A. Walsh, K.-S. Ahn, S. Shet, M. N. Huda, T. G. Deutsch, H. Wang, J. A. Turner, S.-H. Wei, Y. Yan, and M. M. Al-Jassim Energy Environ. Sci. **2**, 774 (2009).